Surface Monitoring of Microseismicity at the Decatur, Illinois, CO_2 Sequestration Demonstration Site

by J. O. Kaven, S. H. Hickman, A. F. McGarr, and W. L. Ellsworth

INTRODUCTION

Sequestration of CO_2 into subsurface reservoirs can play an important role in limiting future emission of CO_2 into the atmosphere (e.g., Benson and Cole, 2008). For geologic sequestration to become a viable option to reduce greenhouse gas emissions, large-volume injection of super-critical CO_2 into deep sedimentary formations is required. These formations offer large pore volumes and good pore connectivity and are abundant (Bachu, 2003; U.S. Geological Survey Geologic Carbon Dioxide Storage Resources Assessment Team, 2013). However, hazards associated with injection of CO_2 into deep formations require evaluation before widespread sequestration can be adopted safely (Zoback and Gorelick, 2012). One of these hazards is the potential to induce seismicity on pre-existing faults or fractures. If these faults or fractures are large and critically stressed, seismic events can occur with magnitudes large enough to pose a hazard to surface installations and, possibly more critical, the seal integrity of the cap rock.

The Decatur, Illinois, carbon capture and storage (CCS) demonstration site is the first, and to date, only CCS project in the United States that injects a large volume of supercritical CO_2 into a regionally extensive, undisturbed saline formation. The first phase of the Decatur CCS project was completed in November 2014 after injecting a million metric tons of supercritical CO_2 over three years. This phase was led by the Illinois State Geological Survey (ISGS) and included seismic monitoring using deep borehole sensors, with a few sensors installed within the injection horizon. Although the deep borehole network provides a more comprehensive seismic catalog than is presented in this paper, these deep data are not publically available. We contend that for monitoring induced microseismicity as a possible seismic hazard and to elucidate the general patterns of microseismicity, the U.S. Geological Survey (USGS) surface and shallow borehole network described below provides an adequate event detection threshold.

The formation targeted for injection is the Mount Simon Sandstone, which is laterally extensive, has high porosity and permeability and has the potential to host future CCS projects due to its favorable hydrologic characteristics and proximity to industrial sources of CO_2 (Birkholzer and Zhou, 2009). At Decatur, CO_2, a byproduct of ethanol production at the Archer Daniels Midland (ADM) facility, is compressed to supercritical state and injected at 2.1 km depth into the 460 m thick Mount Simon Sandstone. This sandstone has varying properties, ranging from the lower, fine- to coarse-grained sandstone with high permeability and porosity, to the middle and upper Mount Simon, which consist of planar, cross-bedded layers of varied permeability and porosity (Leetaru and Freiburg, 2014). The changes in permeability and porosity within the Mount Simon Sandstone, due to depositional and diagenetic differences, create horizontal baffles, which inhibit vertical flow and restrict the injected CO_2 to remain near the injection horizon (Bowen *et al.*, 2011). The lowest portion of the Mount Simon Sandstone overlying the Precambrian rhyolite basement is the Pre-Mount Simon interval, generally <15 m in thickness and composed of fine- to medium-grain size sandstone that is highly deformed (Leetaru and Freiburg, 2014). The basement rhyolite has a clay-rich matrix and is fractured, with significant alterations within the fractures. The primary sealing cap rock is the Eau Claire Formation, a 100–150 m thick unit at a depth of roughly 1.69 km (Leetaru and Freiburg, 2014). The Maquoketa Shale Group and the New Albany Shale serve as secondary and tertiary seals at shallower depths of ~820 and ~650 m, respectively.

The ISGS managed the Illinois Basin–Decatur Project (IBDP), a three-year project beginning in November 2011, during which carbon dioxide was injected at a rate of ~1000 metric tons per day until November 2014 (Finley *et al.*, 2011, 2013). ADM manages the Illinois Industrial CCS (ICCS) project, which will inject ~3000 metric tons/day into a second injection well starting in the summer of 2015.

The USGS began monitoring microseismicity with a 13-station seismic network at Decatur in July 2013 (Fig. 1). This network provides good detection capabilities and azimuthal (focal sphere) coverage for microseismicity with moment magnitudes (M_w) above about −0.5. Here, we report on 19 months of microseismicity monitoring at the Decatur CO_2 sequestration site, which permits a detailed look at the evolution and character of injection-induced seismicity.

NETWORK AND METHODS

Twelve of the USGS seismic stations were installed between July and August 2013, with the 13th station installed on 18 December 2014. Of the 13 stations in the network, nine are equipped with both a three-component broadband seismometer and a

doi: 10.1785/0220150062

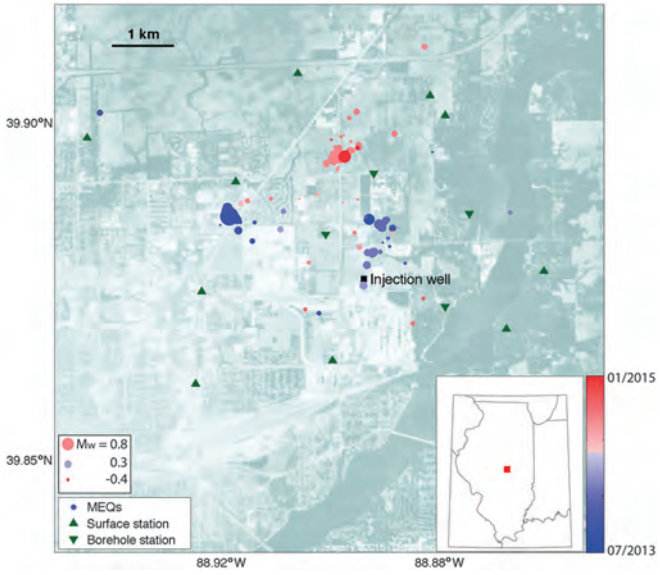

▲ **Figure 1.** Map of U.S. Geological Survey (USGS) Decatur seismic network (green triangles upward for surface-only installations, downward for borehole and surface installations). The carbon capture and storage (CCS) number 1 injection well (black square) and seismicity (dots) scaled by moment magnitude ($-1.13 < M_w < 1.26$) and color coded by event time (locations in World Geodetic System 1984 [WGS84]) are also shown. The inset shows the map location (red square). Air photo (from Google Earth) is included for reference but is not orthorectified.

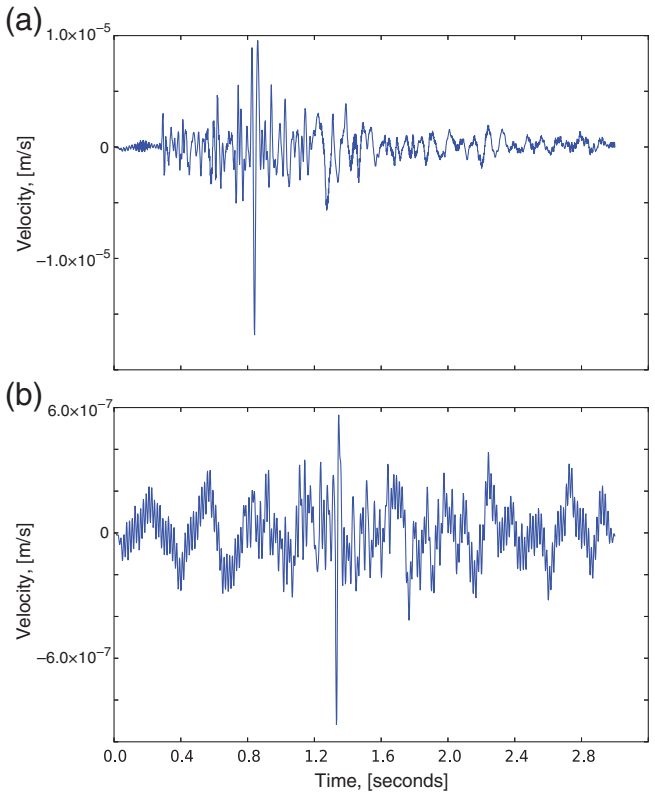

▲ **Figure 2.** (a) Velocity trace from the vertical shallow borehole channel at station DEC03 for an event with M_w 0.86, with instrument response removed. (b) Velocity trace from the vertical shallow borehole channel at DEC03 for an event with M_w 0.23, with instrument response removed and band-pass filtered from 1.0 to 55 Hz.

three-component force-balance accelerometer installed at the surface. At four of the stations, there are three-component force-balance accelerometers at the surface and three-component, high-sensitivity geophones installed in ~150 m deep boreholes. Data are continuously recorded and archived, for public access, at the Incorporated Research Institutions for Seismology Data Management Center. The network has an aperture of roughly 8 km centered on the CO_2 injection well CCS number 1, with the four stations that include borehole sensors located nearest to the well (Fig. 1).

Event detection was carried out using manual inspection of spectrograms to discern small-magnitude events. Manual inspection is necessary due to the low signal-to-noise ratio (Fig. 2). Local sources of noise near the network include the nearby ADM and Caterpillar industrial plants. Since July 2013, we have detected 221 events and located 179 of them, ranging in moment magnitude (M_w) from −1.13 to 1.26. We locate events using the standard Geiger method to determine absolute hypocentral locations (Klein, 1988) and generally achieve nominal absolute location uncertainties < 80 m horizontally and 100 m vertically for events with $M_w > 0$. We calculate M_w by integrating the first displacement pulses of the *P*- and *S*-wave arrivals using source velocities from our 1D model (Fig. 3), calibrated by analyzing a synthetic source at a depth close to the majority of events (Boatwright, 1980; Prejean and Ellsworth, 2001).

Reliable event locations, especially depths, are critically dependent on an accurate velocity model (Kissling *et al.*, 1994). We derived a 1D velocity model using a zero-offset vertical seismic profile (VSP) obtained by ADM and the ISGS in well CCS number 1. We removed outliers and filtered the raw data using a moving average to achieve a less spurious differentiated velocity and fitted piecewise constant segments to the differentiated continuous velocity measurements (Fig. 3b) using fixed-width windows that roughly correspond to 140 m thick layers. We augmented the 1D velocity model with a shallow (< 150 m) acoustic *P*-wave log from USGS borehole DEC02. For the rhyolitic basement, we use velocities of Shelander (2013) to include a semi-infinite basement layer starting at 2.13 km depth. We simplified our velocity model slightly when adjacent layers exhibited similar velocities by averaging the layer velocities (compare to Fig. 3b and c, 1520–1870 m depth); in this way, we minimized numerical instabilities in the ray path calculations, which can arise due to velocity reductions with increasing depth (Lahr, 1999).

We observe velocity inversions at depths of 970, 1520, and 1885 m. We constrain the ratio of *P*- to *S*-wave velocities by simultaneously inverting for microseismic event locations and *P*- and *S*-velocity structure using a subset of microseismic events and arrive at a V_P/V_S ratio of 1.83 (see Kissling *et al.*, 1994). Although somewhat larger than the often-assumed V_P/V_S ratio of 1.73 (corresponding to a Poisson's ratio $\nu = 0.25$), it is sim-

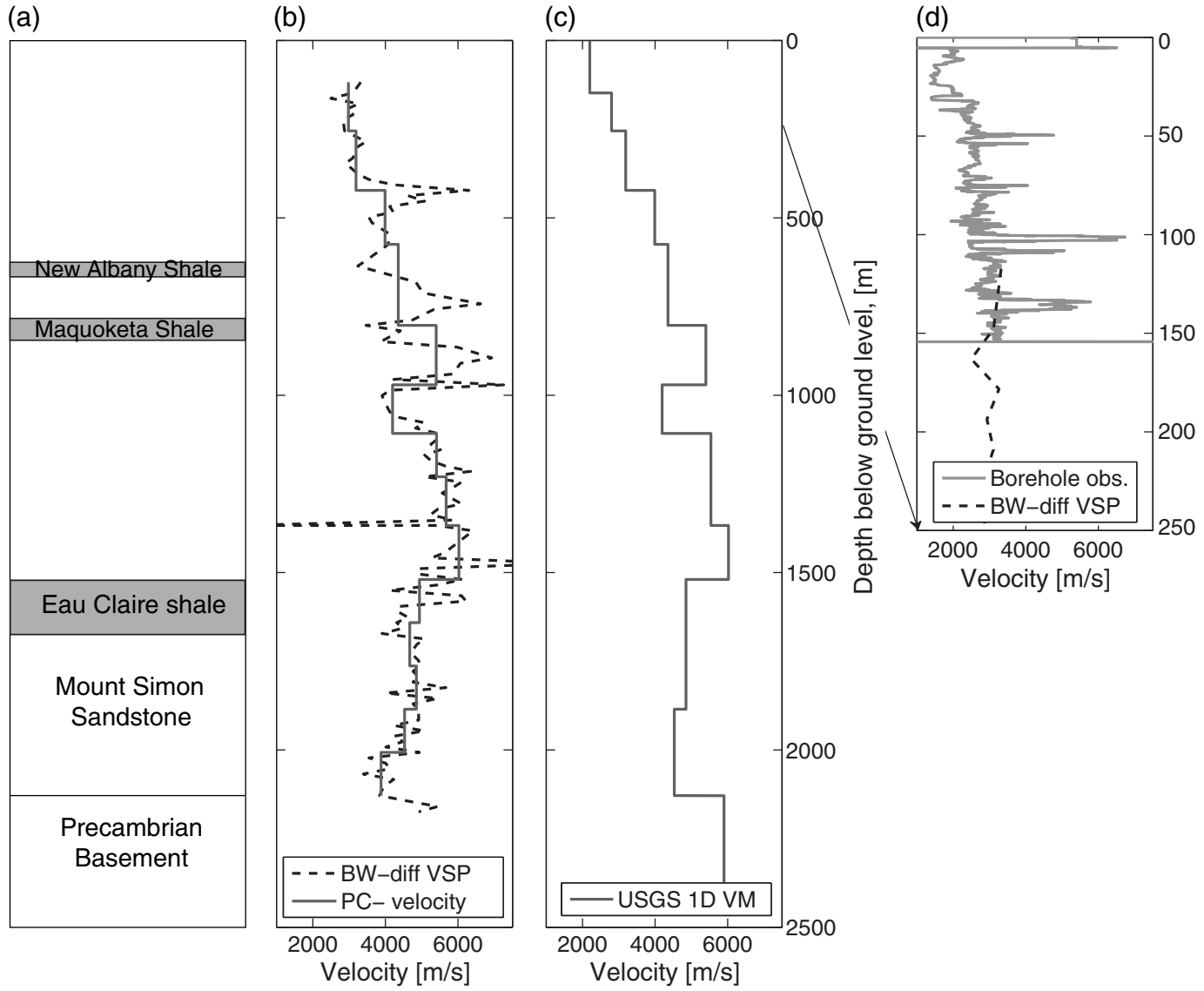

▲ **Figure 3.** (a) Simplified stratigraphy at the Decatur CCS number 1 well with primary and secondary seals indicated by gray horizons. (b) Velocity estimates from backward-difference (BW-diff) and piecewise-constant (PC) fitting to the vertical seismic profile (VSP) run in this well. (c) 1D velocity model adapted from piecewise-constant fit, with granite basement velocity (<2.13 km) from Shelander (2013) and shallow velocities (<150 m) from USGS acoustic *P*-wave log in borehole DEC02. (d) Comparison of acoustic *P*-wave log from DEC02 and shallow portion of backward-differenced VSP data. Note different depth scales in (a) or (b) or (c), and (d).

ilar to ratios commonly observed in sedimentary sequences, especially those that include siltstone and shale (Picket, 1963; Willman *et al.*, 1975).

For a subset of events, we are able to estimate focal mechanisms using the *P*-wave polarities from at least eight network stations. We find focal mechanisms most consistent with first motions by grid searching over the entire solution space and selecting only those mechanisms that have the highest probability per event (Hardebeck and Shearer, 2002). We choose large azimuthal and take-off angle gap criteria (120° and 85°, respectively) in the calculations owing to the relatively small magnitudes of these events and the locations of microseismicity clusters within our network that limit the variety of first motions detected.

RESULTS

Hypocenters located at Decatur primarily fall into three distinct clusters (Fig. 1). One cluster at and immediately to the north of the injection well (east cluster) extends to the north-northeast for about 1.0 km. This cluster has been active since the start of USGS network operations. A second cluster at a distance of about 2.0 to 2.6 km northwest from the injection well was active for roughly three weeks in September of 2013 and includes only few events. The most recently active cluster is located to the north of the injection well, at distances between 1.8 and 2.3 km, with the first events detected in July of 2014. Each cluster includes events with M_w ranging from −0.5 to at

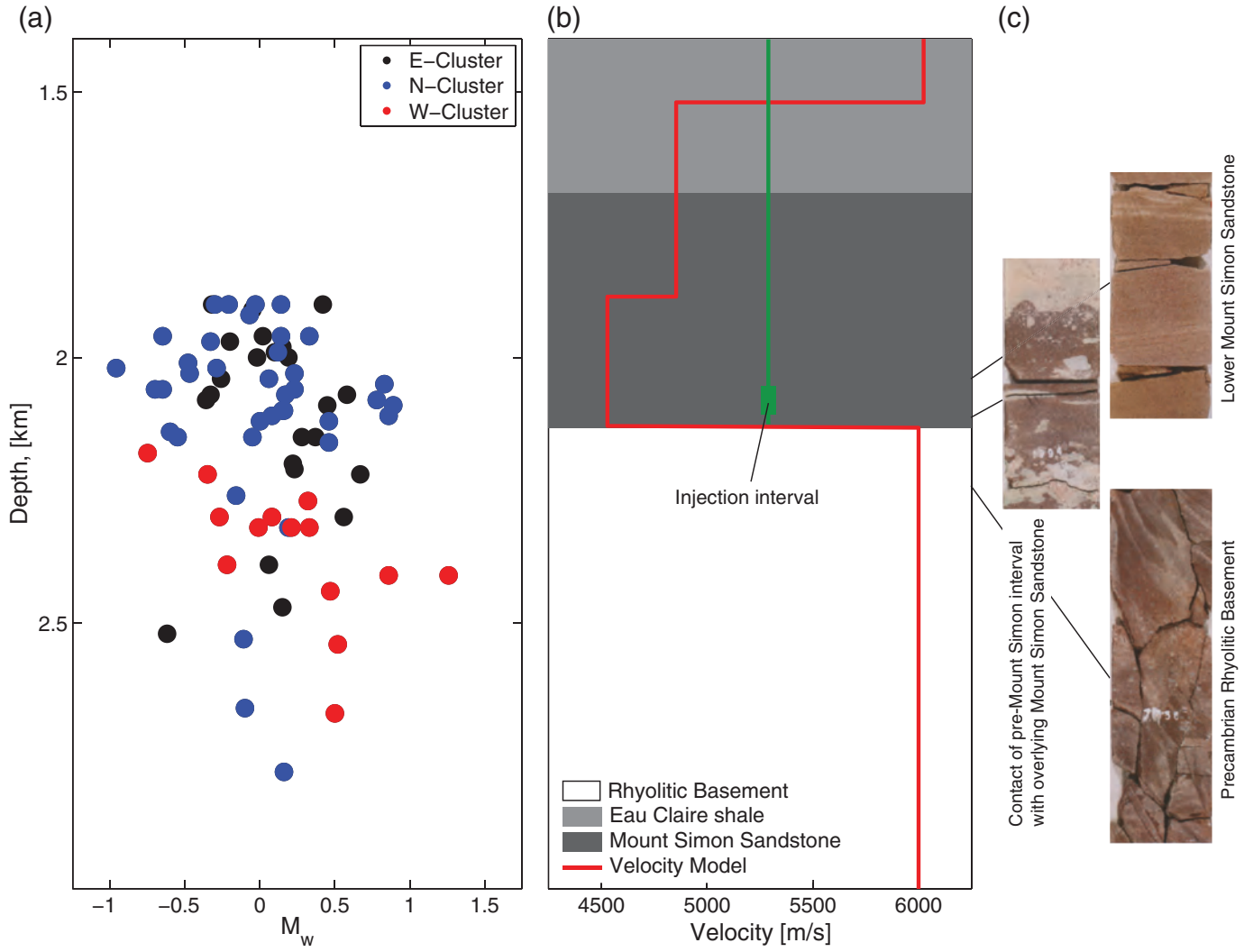

▲ **Figure 4.** (a) Depth versus M_w for the three separate clusters shown in Figures 1 and 5, in which symbols are color-coded by cluster and not sized by event magnitude. Events with nominal vertical location errors of <500 m only are shown here (see text for discussion of event depths and uncertainties). (b) Simplified stratigraphic profile showing the CO_2 storage unit (Mount Simon Sandstone) in relation to the primary cap rock (Eau Claire Shale), with the 1D velocity model and injection well superimposed. Note that depth in both panels starts at 1.4 km. (c) Core images from the lower Mount Simon Sandstone, the Pre-Mount Simon Sandstone in contact with the lower Mount Simon, and the Precambrian rhyolite basement from Leetaru and Freiburg (2014).

least 0.8, absolute hypocentral depths between 1.9 and 2.7 km, and the large majority of all events are within 200 m of the basement-Mount Simon contact (Fig. 4). All events are thus located in the lower Mount Simon Sandstone, the Pre-Mount Simon Sandstone or in the Precambrian basement and at least 200 m below the Eau Claire Shale cap rock. Events with $M_w \geq 0.5$ show a similar depth distribution but are at least 400 m below the Eau Claire Shale cap rock. The eastern and northern clusters have comparable source depths, whereas events in the western cluster tend to be deeper.

We refine the locations of a subset of events by relocating these with double-difference methods using differential travel times from phase picks and waveform cross correlations to achieve high-precision relative locations (Waldhauser and Ellsworth, 2002). We used all waveform pairs with cross-correlation coefficients > 0.7 and damp the solution to achieve a good compromise between retaining the maximum number of events while also reducing the root mean square errors in the locations. Of the initial 179 events, we retain 66 in the final relocated catalog. We lost a large number of small magnitude events due to significant, nonstationary noise that prohibit cross correlation of waveforms. The resulting relocations yielded improved definition of the clusters, in particular for the central cluster nearest the injection well. This cluster forms a roughly linear pattern with a north-northeast trend (Fig. 5). The western cluster sharpens slightly with a faint trend from west-northwest to east-southeast, but the pattern is not as distinct and linear as for the central cluster. The northern cluster also sharpens slightly, but a clear

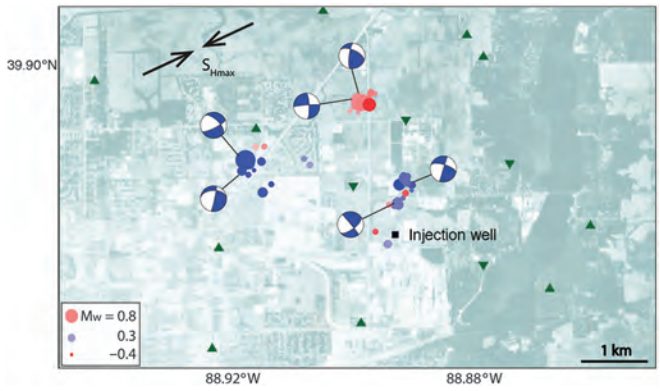

▲ **Figure 5.** Double-difference relocated microseismicity using differential travel times from phase arrival times and waveform cross correlation (correlation coefficient ≥0.7, see text for details). Focal mechanisms are from *P*-wave polarity for six events. Regional orientation of the maximum horizontal principal stress (SH_{max}) is indicated by opposing arrows (Nelson and Bauer, 1987). Symbols scaled to M_w and color-coded by origin time, as in Figure 1. Air photo (from Google Earth) is included for reference but is not orthorectified.

lineation is not readily apparent. Hypocentral depths after relocation remain in the same depth range as for the absolute depths, extending from about 1.9 to 2.7 km. Further, the relative locations shift by <120 m horizontally and 140 m vertically from the absolute locations, suggesting that our actual location errors for events with $M_w > 0.5$ are, in fact, of the order of 120 m horizontally and 140 m vertically.

Six focal mechanisms indicate right-lateral strike slip to oblique strike-slip mechanisms (Fig. 5). Strike orientations range from 331° to 063, with an average strike of 22°. The dip ranges between 62° and 90°, with an average dip of 75°. Similarly, the average rake is −148°, ranging from −121° to −172°, indicating oblique strike-slip relative motion. Thus, the axis of compression is oriented east-northeast to west-southwest. The regional maximum horizontal principal stress from borehole measurements (Nelson and Bauer, 1987) is oriented at 062°, which is consistent with the focal mechanisms at all three clusters (Fig. 5).

DISCUSSION AND CONCLUSIONS

For CCS to become a viable option in reducing greenhouse gas emissions, vast amounts of CO_2 require long-term geological sequestration. The candidates for CCS with the greatest storage capacity nationwide are saline aquifers like the Mount Simon studied here, which provide horizontally extensive, high-porosity, high-permeability reservoirs (U.S. Geological Survey Geologic Carbon Dioxide Storage Resources Assessment Team, 2013). Many of these formations are similar to the Mount Simon in that they overlie Precambrian basement. Extensive implementation of CCS in such formations would increase the likelihood of encountering unmapped, near critically stressed faults capable of producing earthquakes large enough to pose a hazard to surface installations and sealing cap integrity (Zoback and Gorelick, 2012). At Decatur, however, no felt seismicity or seismicity greater than M_w 1.26 has been observed, despite injecting roughly one million metric tons of super-critical CO_2.

Microseismicity at Decatur tends to cluster, and these clusters do not appear to be at distances from the injection well that are monotonically increasing with time. This pattern of seismicity indicates heterogeneous pore pressure redistribution that is likely the result of an inhomogeneous and perhaps anisotropic permeability structure. Depositional changes and fractures are clearly visible in core samples from wells at the Decatur site, particularly from the basement rhyolite (Leetaru and Freiburg, 2014). Both the alignment of clusters after relocation and the focal mechanisms of a subset of events suggest that microseismicity in the basement may nucleate on pre-existing faults that are well oriented with respect to the regional stress field. These pre-existing fault zones may further provide high-permeability channels for the injected fluid. We suggest that alternating low-permeability horizons limit vertical flow within the Mount Simon Sandstone (Bowen *et al.*, 2011) and, possibly in concert with aligned faults and fractures in the lower Mount Simon, Pre-Mount Simon and basement, create a heterogeneous flow field that aids in localizing microseismicity largely at depths ranging from the injection interval to the upper part of the basement. This permeability structure likely also prevents significant pore pressure communication into the upper Mount Simon and near the primary seal, the Eau Claire Shale.

We thus conclude that current microseismicity detected at the Decatur site is unlikely to pose a hazard to the integrity of the Eau Claire Shale, due to the significant distances of the hypocenters from the seal and the low observed magnitudes of these events. Although detected seismicity at Decatur is of low magnitude, we note the Decatur site shares many characteristics of other injection-induced seismicity locales that have experienced seismicity of greater magnitudes and consequences (e.g., Kim, 2013). Much more research is required at the Decatur CCS project to understand the relationship between long-term injection and induced seismicity there. The forthcoming additional findings from the Illinois Basin–Decatur Project (IBDP) and work conducted by the ISGS and the future ICCS project at Decatur will provide an excellent opportunity for this.

ACKNOWLEDGMENTS

We appreciate the discussions with Scott McDonald (Archer Daniels Midland), Robert Finley and Robert Bauer (Illinois State Geological Survey), and Robert Will and Paul Jacques (Schlumberger Carbon Services). We also appreciate thorough reviews by Jeanne Hardebeck, David Shelly, and Keith Knudsen (U.S. Geological Survey), and two anonymous reviewers. Any use of trade, firm, or product names is for descriptive purposes only and does not imply endorsement by the U.S. Government.

REFERENCES

Bachu, S. (2003). Screening and ranking of sedimentary basins for sequestration of CO_2 in geological media in response to climate change, *Environ. Geol.* **44,** no. 3, 277–289, doi: 10.1007/s00254-003-0762-9.

Benson, S. M., and D. R. Cole (2008). CO_2 sequestration in deep sedimentary formations, *Elements* **4,** no. 5, 325–331.

Birkholzer, J. T., and Q. Zhou (2009). Basin-scale hydrogeologic impacts of CO_2 storage: Capacity and regulatory implications, *Int. J. Greenh. Gas Control* **3,** 745–756, doi: 10.1016/j.ijggc.2009.07.002.

Boatwright, J. (1980). A spectral theory for circular seismic sources: Simple estimates of source dimension, dynamic stress drop, and radiated seismic energy, *Bull. Seismol. Soc. Am.* **10,** no. 1, 1–17.

Bowen, B. B., R. I. Ochoa, N. D. Wilkens, J. Brophy, T. R. Lovell, N. Fischietto, C. R. Medina, and J. A. Rupp (2011). Depositional and diagenetic variability within the Cambrian Mount Simon Sandstone: Implications for carbon dioxide sequestration, *Environ. Geosci.* **18,** no 2, 69–89.

Finley, R. J., S. M. Frailey, H. E. Leetaru, O. Senel, M. L. Coueslan, and S. Marsteller (2013). Early operational experience at a one-million Tonne CCS demonstration project, Decatur, Illinois, USA, *Energy Procedia* **37,** 6149–6155, doi: 10.1016/j.egypro.2013.06.544.

Finley, R. J., S. E. Greenberg, S. M. Frailey, I. G. Krapac, H. E. Leetaru, and S. Marsterller (2011). The path to a successful one-million tonne demonstration of geological sequestration: Characterization, cooperation, and collaboration, *Energy Procedia* **4,** 4770–4776, doi: 10.1016/j.egypro.2011.02.441.

Hardebeck, J. L., and P. M. Shearer (2002). A new method for determining first motion focal mechanisms, *Bull. Seismol. Soc. Am.* **92,** 2264–2276.

Kim, W.-Y. (2013). Induced seismicity associated with fluid injection into a deep well in Youngstown, Ohio, *J. Geophys. Res.* **118,** 3506–3518, doi: 10.1002/jgrb.50247.

Kissling, E., W. L. Ellsworth, D. Eberhart-Phillips, and U. Kradolfer (1994). Initial reference models in local earthquake tomography, *J. Geophys. Res.* **99,** no. B10, 19635–19646.

Klein, F. W. (1988). User's guide to HYPOINVERSE, a program for VAX computers to solve for earthquake locations, *U. S. Geol. Surv. Open-File Rept. 88*.

Lahr, J. C. (1999). Revised 2012, HYPOELLIPSE: A computer program for determining local earthquake hypocentral parameters, magnitude, and first-motion pattern, *U.S. Geol. Surv. Open-File Rept. 99-23*, version 1.1, 119 pp., and software, available at http://pubs.usgs.gov/of/1999/ofr-99-0023/ (last accessed January 2014).

Leetaru, H. E., and J. T. Freiburg (2014). Litho-facies and reservoir characterization of the Mt Simon Sandstone at the Illinois Basin–Decatur Project, *Greenhouse Gases: Science and Technology* **4,** no. 5, 580–595.

Nelson, W. J., and R. A. Bauer (1987). Thrust faults in the Illinois basin—Result of contemporary stress? *Geol. Soc. Am. Bull.* **98,** 302–307.

Picket, G. R. (1963). Acoustic character logs and their applications in formation evaluation: 1, *Can. Petr. Tech.* **15,** 659–667.

Prejean, S., and W. L. Ellsworth (2001). Observations of earthquake source parameters at 2 km depth in the Long Valley Caldera, Eastern California, *Bull. Seismol. Soc. Am.* **91,** no. 2, 165–177.

Shelander, D. (2013). 3D seismic at Illinois basin–Decatur Project revisited, *Midwest Carbon Sequestration Science Conference*, Champaign, Illinois, 7 October 2013.

U.S. Geological Survey Geologic Carbon Dioxide Storage Resources Assessment Team (2013). National assessment of geologic carbon dioxide storage resources—Results (ver. 1.1, September 2013), *U.S. Geol. Surv. Circular 1386*, 41 pp., http://pubs.usgs.gov/circ/1386/ (last accessed October 2014) (Supersedes ver. 1.0 released 26 June 2013).

Waldhauser, F., and W. L. Ellsworth (2002). Fault structure and mechanics of the Hayward fault, California, from double-difference earthquake locations, *J. Geophys. Res.* **107,** doi: 10.1029/2000JB000084.

Willman, H. B. E., T. Atherton, T. C. Buschnach, C. Collinson, J. C. Frye, M. E. Hopkins, J. A. Lineback, and J. A. Simon (1975). *Handbook of Illinois Stratigraphy*,Illinois State Geological Survey, Champaign, Illinois, Bulletin, Vol. 95, 261 pp.

Zoback, M. D., and S. M. Gorelick (2012). Earthquake triggering and large-scale geologic storage of carbon dioxide, *Proc. Natl. Acad. Sci. Unit. States Am.* **109,** doi: 10.1073/pnas.1202473109.

J. O. Kaven
S. H. Hickman
A. F. McGarr
W. L. Ellsworth
USGS Earthquake Science Center
Menlo Park, California 94025 U.S.A.
okaven@usgs.gov